TESTING THE INVERSE BORN PROCEDURE FOR SPHEROIDAL VOIDS*

J. H. Rose
Physics Department
University of Michigan
Ann Arbor, Michigan 48109

V. V. Varadan and V. K. Varadan
Boyd Laboratory
Ohio State University
Columbus, Ohio 43210

R. K. Elsley and B. Tittman
Rockwell International Science Center
Thousand Oaks, California 91360

ABSTRACT

Previously we have shown that the inverse Born approximation allows an accurate determination of the radius of spherical flaws in Ti. Here we report the results of extending that analysis to spheroidal voids. Both oblate and prolate spheroids are considered. Using scattering amplitude generated by the T-matrix method, we find that both the major and minor axes of 2-1 spheroids are accurately determined. Inversion results using experimental data will be presented for the 2-1 oblate spheroid: a comparison of the experimental and theoretical results will be given.

INTRODUCTION

Recent developments in ultrasonic scattering theory have been strongly motivated by the nondestructive evaluation needs of the structural materials community. Their primary question is; given a set of ultrasonic measurements (e.g. scattering amplitudes) from some industrial component, when will it break? An intermediate step in answering this question is: given the scattering data, what are the characteristics of the flaws in the piece? Here one would like to know if one has a volume flaw such as a void or inclusion, or if one has a crack. Also, one would like to know the size, shape and orientation of the flaw: and, if it is an inclusion, what it is made of. Answering these questions is what I will refer to as the ultrasonic inversion problem.

The current status of the ultrasonic inversion problem depends upon the ratio of the characteristic size of the flaw (a_o) to the wavelength λ ($k = 2\pi/\lambda$). When the size of flaw is much larger than the wavelength, $ka_o >> 1$, then imaging techniques can be used, and a good deal of progress has been made. In the opposite limit, $ka_o << 1$, there has been some recent progress, both in terms of describing what information can be extracted in principle and in terms of practical algorithms for simply shaped flaws.[1] Between these two limits we have the intermediate regime, where the wavelength is on the order of the size of the object. This paper focuses on the intermediate regime and studies the geometric features of single voids.

We will review the theoretical development of an inversion algorithm for the intermediate wavelength case.[2] Further, we will summarize the progress of our group effort to empirically verify this algorithm. The need for detailed empirical verification stems from the theoretical justification of the algorithm, which is based on perturbative solutions of the wave equation and is valid only if the scattering is sufficiently weak! However, many of the flaws of interest in NDE are anything but weak (e.g. a void). It is not clear how to extend our current inversion algorithm formally to the strong scattering case. However, for voids of simple shape, the algorithm yields good results as we will report.

It is in this empirical verification scheme that recent developments in elastic wave scattering theory (such as the T-matrix method[3]) have a key role to play. For in order to establish the limits of validity of this algorithm and other empirical inversion algorithms, it is desirable to have the scattering amplitudes for a wide range of differently shaped flaws. Particularly interesting for this purpose would be flaws with sharp edges such as cones and pill boxes. Up to the present time we are limited to investigating spherical, and oblate and prolate spheroidal flaws.

The structure of the paper is as follows. In the second section we review the derivation of the algorithm. In section three we indicate how the theory was simplified for the case of ellipsoidally shaped flaws. In the fourth section we report the results of testing the algorithm with experimentally generated data. In the fifth section we report the results of testing the inversion algorithm using scattering amplitudes generated by the T-matrix method for 2-1 oblate and prolate spheroidal voids. Finally, in section six we provide a discussion of our results and conclude.

GENERAL THEORY

The algorithm to be discussed below is a procedure for approximately determining the Fourier transform of the characteristic function, $\gamma(\vec{r})$, of the flaw. Here $\gamma(\vec{r})$ is 1 for $\vec{r}$ inside the flaw, and $\gamma(\vec{r})=0$ for $\vec{r}$ outside the flaw. We restrict our review of the theory to the simplest experimental situation. That is we assume a pulse-echo geometry as shown in Fig. 1. Here a longitudinally or shear polarized plane wave is incident on the

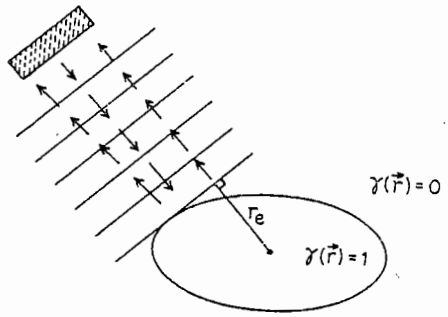

Figure 1. The geometry of a pulse echo experiment. The distance from the center of the flaw to the tangent plane is the effective radius, r_e, discussed in the text.

flaw, and the directly backscattered longitudinal or shear amplitude is determined. The pulse echo scattering amplitudes can be written for an arbitrarily shaped flaw as

$$A(\vec{k}) = a(\vec{k},\{\mu\})S(2\vec{k})k^2 \qquad (2\text{-}1)$$

Here $S(2\vec{k})$, the shpae factor, is the Fourier transform of the characteristic function of the flaw. The wavevector of the incident wave is denoted by $\vec{k}$ and $a(\vec{k},\{\mu\})$ is a function to be calculated which yields the correct scattering amplitudes A for an arbitrary $\vec{k}$. Here $\{\mu\}$ denotes the material parameters of the host material.

The virtue of writing the scattering amplitudes in the form of Eq. 2.1 is that several approximate theories[4,5] yield very simple forms for the factor $a(\vec{k},\{\mu\})$. In particular we will use the form of $a(\vec{k},\{\mu\})$ which can be derived from the extended quasi-static approximation. In that approximation one takes account of the long wavelength elastic deformation of the flaw correctly, and hence obtains the angular features of the scattering correctly in this limit. For the extended quasi-static approximation $a(\vec{k},\{\mu\})$ is assumed to be independent of $|\vec{k}|$ and given by its long wavelength limit which depends only on the direction of $\vec{k}$, $\hat{k}$, and on $\{\mu\}$. We denote this approximate form of $a(\vec{k},\{\mu\})$ as $a_{QSA}(\hat{k},\{\mu\})$. Using this approximation we rewrite equation 2.1 as

$$S(2\vec{k}) \simeq A(\vec{k})/(k^2 a_{QSA}(\hat{k},\{\mu\})) \qquad (2.2)$$

Experimentally, a_{QSA} can be obtained for an arbitrarily shaped object by measurements of the long wavelength scattering amplitudes. In that limit $S(2\vec{k})$ goes to a constant, and a_{QSA} can be determined from the angularly dependent coefficients of A

$$a_{QSA}(\hat{k},\{\mu\}) = \lim_{k\to 0} A(\vec{k})/k^2 \qquad (2.3)$$

Once a_{QSA} is obtained we can determine $S(2\vec{k})$ from Eq. 2.3 via an experimental measurement of the backscattered amplitudes. Taking the Fourier transform of $S(2\vec{k})$ then allows us to determine the characteristic function of the flaw, and hence its size, shape and orientation. The major approximation in using a_{QSA} is that we assume that it depends only on $\hat{k}$ and not on $|\vec{k}|$. The characteristic function is given explicitly in terms of the shape function as[6]

$$\gamma(\vec{r}) = \text{const.} \int d^3\vec{k}\, e^{2i\vec{k}\cdot\vec{r}}\, R_e(A(\vec{k}))/(k^2\, a_{QSA}(\hat{k},\{\mu\})) \qquad (2.4)$$

SIMPLIFIED THEORY FOR ELLIPSOIDALLY SHAPED FLAWS

In the last section we described an approximat procedure for determining the size, shape and orien tation of an arbitrary three dimensional flaw. In order to use this inversion technique one requires pulse-echo measurements from all incident direction $\hat{k}$. The characteristic function is then obtained (Eq. 2.4) as an inverse Fourier transform which involves integrating over both $|\vec{k}|$ and $\hat{k}$. For the class of ellipsoidally shaped flaws, one can obtain all relevant information about the flaw by invertin each pulse-echo record independently as discussed below. This avoids the angular integration over k in the inverse Fourier transform, and significantly simplifies the application of the algorithm.

In order to illustrate how this simplification comes about, let us consider the weak scattering limit. Then the theory of the last section is rigorously valid and Eq. 2.2 becomes

$$S(2\vec{k}) = \text{const.}\, A_{L\to L}(\vec{k})/\, k^2 \qquad (3.1)$$

We have used the fact that $a(\hat{k},\{\mu\})$ is a constant in the weak scattering limit as a function of $\hat{k}$. For an ellipsoid we know that $S(2\vec{k})$ is given by the following equations

$$S(2k) = \frac{\sin(2\,k\,r_e) - 2\,k\,r_e\cos(2\,k\,r_e)}{(2\,k\,r_e)^3} \qquad (3.2)$$

and

$$r_e = (a_x^2\cos^2\theta\sin^2\phi + a_y^2\cos^2\theta\cos^2\phi + a_z^2\sin^2\theta)^{1/2} \qquad (3.3)$$

Here the axes of the ellipsoid are $a = (a_x, a_y, a_z)$, and θ and ϕ define the direction of $\hat{k}$ in spherical co-ordinates. The angular dependence of the shape factor comes in strictly through the function which we have called $r_e(\theta,\phi)$. In a pulse-echo measurement, the incident direction $\hat{k}$ is kept fixed, and r_e is a constant for that set of data. We note for a fixed incident direction, Eq. 3.2 has the same form as a Fourier transform of a sphere with an effective radius r_e. For each incident direction $\hat{k}$, we obtain r_e in the following way. First we obtain $S(2|\vec{k}|)$ from Eq. 3.1. We then extend $S(2|\vec{k}|)$ to be spherically symmetric in k-space. Thus, we obtain the three dimensional Fourier transform of a sphere of radius $r_e(\theta,\phi)$. This Fourier transform is then inverted to yield the effective radius for that direction. The resulting effective radius (Eq. 3.3) has a simple geometric interpretation as shown in Fig. 1. When a wavefront strikes the surface, it is first tangent at some one point (which is an accumulation point for phase). The radius r_e is the distance from the center of the

flaw to the plane of the wavefront. An important consequence of Eq. 3.3 is that pulse-echo measurements along the axis of an ellipsoid yield the axis length directly. For example, a measurement along the a_x axis yields an effective radius equal to a_x. Hence, one can obtain the length of the ellipsoid axes directly from three measurements if one knows the orientation of the ellipsoid.

So far we have been discussing the weak scattering limit for the sake of illustration. The appropriate extension to the strong scattering case is straightforward. Eq. 2.2 is

$$S(2k) \approx \text{const. } A(\vec{k})/(k^2 a_{QSA}(\hat{k},\{\mu\})) \qquad (3.4)$$

For a given incident direction $a(\hat{k},\{\mu\})$ is just a constant since it doesn't depend on $|\vec{k}|$ in the quasi-static approximation. With this approximation we recover Eq. 3.1 and can proceed in an approximate way with the entire procedure which was given above. Of course for a strongly scattering flaw, our analysis is only approximate and must be checked empirically. In the next sections we provide some empirical tests of the strong scattering limit.

INVERSION OF EXPERIMENTAL DATA

We summarize the initial results of testing the algorithm, in its simplified form for ellipsoids, with experimental data. More extensive results and a comprehensive treatment of both experiment and data analysis will be given in Ref. 7. We report results for a spherical void with a radius of 400 microns, and an oblate spheroid with a semi-major axis of 400μ and a semi-minor axis of 200μ. These were machined flaws in the center of large spheres of Ti-6Al-4V. Details of the construction of the flaws and their use as calibration samples are given in Ref. 8 and 9.

The simplified algorithm allows us to treat each pulse-echo measurement separately, and it yields the distance from the center of the flaw to the tangent plane of the incoming wavefront. For the sphere we obtained a single pulse-echo record which suffices to determine the size of the flaw due to its spherical symmetry. However, for the spheroid we only examined the pulse-echo record for a measurement along the axis of symmetry.

Before presenting the results, we want to discuss two crucial details of the data analysis scheme. First, for sufficiently small wavevector, k, the phase of the scattering amplitudes must be constant and zero. This reflects the fact that the real part of the scattering amplitude rises as k^2 for small k while the imaginary rises much more slowly. This constraint on the phase allows one to establish the phase of the experimental data, which otherwise would not be entirely determined.[7] The second point concerns the effects of limited bandwidths. A lack of low frequency data would leave the phase of the data undetermined as just indicated. A lack of high frequency data causes the characteristic function to be blurred, and this introduces some uncertainty in determining the size of the flaw. In large part the effects of blurring due to the limited bandwidth can be overcome by an appropriate calibration procedure. For the simplified form of the algorithm, the analysis is carried out in terms of equivalent spheres. The effects of a limited high frequency bandwidth on the characteristic function of a sphere can be determined in the following way. We consider the Fourier transform of a sphere in k-space. We then band-limit it with a rectangular window extending from k=0 to k_{max}. Then we transform it back to r-space. The resulting curves can then be compared to the experimentally determined characteristic functions and thus serve as a calibration for the effects of blurring.

Inverting the pulse-echo data for the sphere (0<ka<4) where a is the radius. We find a radius of approximately 400μ with an uncertainty of about 40μ. This should be compared to the exact value of 400μ. The inversion of the spheroid data data yields an estimate of the semi-minor axis of 220μ with an uncertainty of about 20μ. The exact value is 200μ. We consider these results to be quite encouraging. It is clear however, that considerably more scattering data for other orientations of the spheroids, for other materials and for other types of volume flaws (e.g. inclusions) will be necessary before the algorithm can be considered fully tested. To partially examine these questions we turn to the theoretically generated data of the next section.

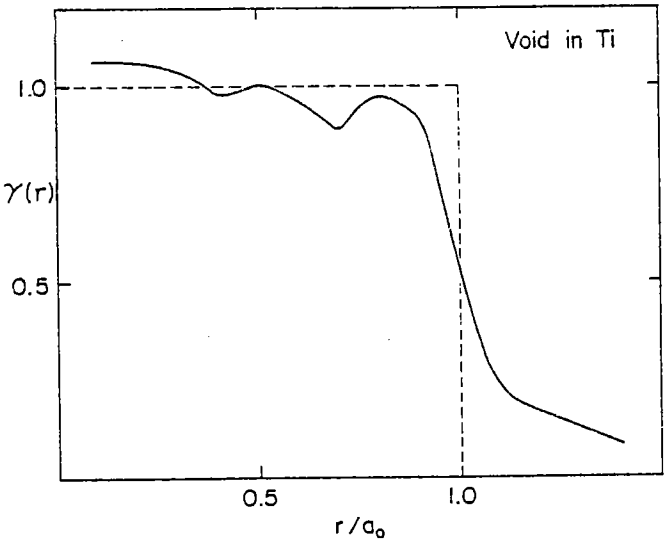

Figure 2. The calculated characteristic function for a spherical void of radius, a, in titanium. The result was obtained by inverting theoretical scattering amplitudes with a bandwidth 0 ka_o 10.

INVERSION OF THEORETICAL DATA

The inversion algorithm was tested for three different flaws in titanium using data generated from theory. The first flaw as a spherical void with 0<ka<10. The second flaw was a 2-1 oblate spheroid with 0<ka<4 (where a denotes the semi-major axis). The third flaw was a 2-1 prolate spheroid with 0<kb<4 (here we define b as the semi-minor axis). The sphere data was generated using the exact theory of Ying and Truell and isotropic elastic constants for titanium. The T-matrix method was used to obtain the scattering apmplitudes for the (400μ by 200μ) prolate and oblate spheroidal flaws.

The spherical flaw is considered first. Figure 2 shows the characteristic function obtained from the inversion procedure. Using the 50% point to define the boundry, we find that the radius is determined to within about 5%. We note that the inversion procedure was tested for sensitivity to noise for this spherical flaw and found to be quite

insensitive.[7]

The preliminary analysis of the spheroidal data is confined to an approximate determination of the semi-major and semi-major axes using the simplified theory of section three. The simplified theory has the feature that a pulse-echo waveform along one of the axes can be used to determine the radius of an equivalent sphere with the radius of that axis. In Fig. 3 we show the characteristic function derived from the pulse-echo waveform measured along the semi-minor axis. Figure 4 is the equivalent

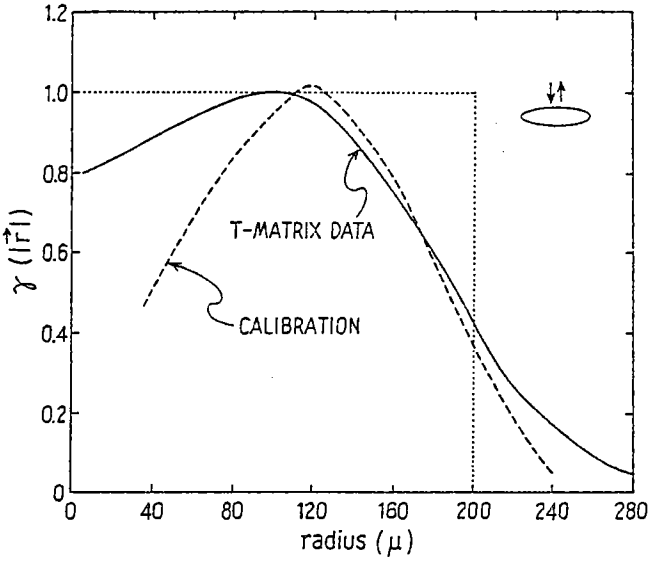

Figure 3. Calculated characteristic function for the semi-minor axis of the prolate spheroid using theory data with a bandwidth of 0<kb<4.

result for the semi-major axis. Using these results we obtain estimates of 420μ and 210μ for these axes compared to the exact results of 400μ and 200μ. Similar results for the oblate spheroids are 360μ and 210μ compared to exact values of 400μ and 200μ.

In section four we calculated the characteristic function for the semi-minor axis of an oblate spheroid from experiment. In this section we computed the same result using scattering amplitudes obtained from the T-matrix method. We now compare both results (with a bandwidth 0<kb<2). The results are shown in Fig. 5, and the agreement is essentially exact.

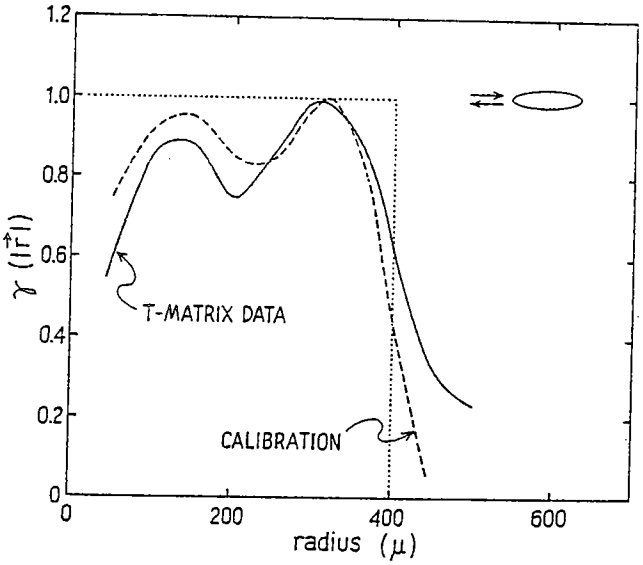

Figure 4. Calculated characteristic function for the semi-major axis of the prolate spheroid using the theory data with a bandwidth of 0<ka<4.

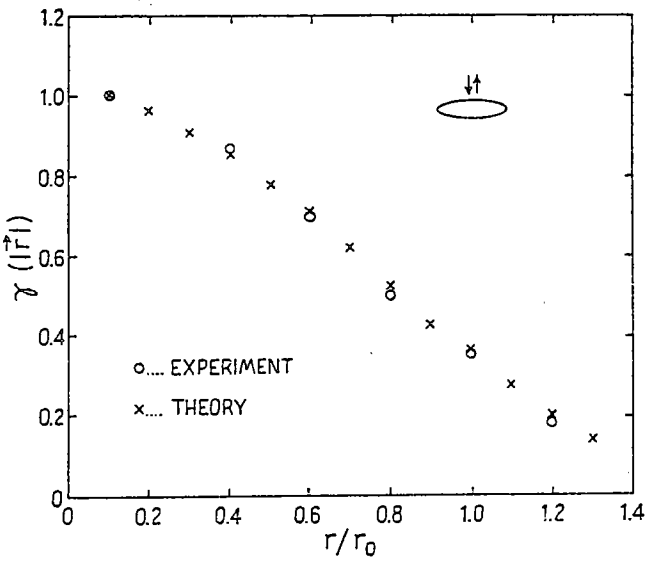

Figure 5. The calculated characteristic functions for the semi-minor axis of the oblate. Theory and experiment are compared.

CONCLUSION

We have presented an inversion algorithm for the intermediate scattering regime when the size of the flaw is comparable to the wavelength of the ultrasound. Tests of the algorithm were performed for the case of spherical and spheroidal voids in Titanium. Good results were obtained for the size and shpae of the flaws. These results suggest that this algorithm may be of practical use for the non-

destructive testing community in determining the characteristics of volume type flaws in various solids.

REFERENCES

*This research was supported by the Center for Advanced NDE, Rockwell International Science Center.

1. J. M. Richardson, IEEE Ultrasonics Symposium, Cherry Hill New Jersey 759 (1978).
2. J. H. Rose and J. A. Krumhansl, J. Appl. Phys. 50 2951 (1979).
3a. V. V. Varadan and Y. H. Pao J. Acoust. Soc. Am. 60 556 (1976).
b. V. V. Varadan J. Acoust. Soc. Am. 63 1014 (1978).
c. V. V. Varadan and V. K. VaradanJ. Acoust. Soc. Am., in press.
4. J. E. Gubernatis, E. Domany, J. A. Krumhansl and M. Huberman, J. Appl. Phys. 48 2812 (1977).
5. J. E. Gubernatis, Los Alamos Scientific Laboratories Report LA-UR-771339 (1977), unpublished.
6. The characteristic function, $\gamma(\vec{\gamma})$, is real which we insure by inverting only the real part of the scattering amplitude. This procedure for preserving the reality of γ is discussed in reference 7.
7. J. H. Rose, V. V. Varadan, V. K. Varadan, R. K. Elsley and B. R. Tittman, to be published.
8. B. R. Tittman, E. R. Cohen, J. M. Richardson, J. Acoust. Soc. Am. 63 68 (1978).
9. B. R. Tittman, R. K. Elsley, H. Nadler and E. R. Cohen, to be published.